Polymorphism in a Metallocenic Isotactic Polypropylene as Revealed by Means of FTIR Spectroscopy: Influence of the Processing Conditions

V. Lorenzo,[1] M.J. Polo-Corpa,[2] E. Pérez,[2] R. Benavente,[2] M.U. de la Orden,[3] J. Martínez-Urreaga[1]

[1]*POLímeros: Caracterización y Aplicaciones (POLCA – UA del ICTP-CSIC), Universidad Politécnica de Madrid, José Gutiérrez Abascal 2, 28006, Madrid, Spain*
[2]*Instituto de Ciencia y Tecnología de Polímeros, CSIC, Juan de la Cierva 3, 28006, Madrid, Spain*
[3]*Depto. de Química Orgánica I, Escuela Universitaria de Óptica, Universidad Complutense de Madrid, Arcos de Jalón s/n, 28037, Madrid, Spain*

Received 14 April 2010; accepted 5 November 2010
DOI 10.1002/app.33707
Published online 25 February 2011 in Wiley Online Library (wileyonlinelibrary.com).

ABSTRACT: The polymorphic structure in specimens of a metallocenic isotactic polypropylene, processed under different conditions, has been studied by means of wide-angle X-ray scattering (WAXS), differential scanning calorimetry (DSC), and Fourier transform infrared spectroscopy (FTIR). The proportions of the different polymorphs have been evaluated, and the influence of the processing parameters (nucleating agents, cooling rate, and nature of the surface of the molds) has been analyzed. The combination of WAXS, DSC, and FTIR results confirms the adequacy of this last technique to obtain quantitative information about the competition between the crystalline phases of polypropylene. It has also been proved that the nature of the mold can enhance considerably the activity of beta-nucleating agents. © 2011 Wiley Periodicals, Inc. J Appl Polym Sci 121: 1023–1031, 2011

Key words: poly(propylene); polymorphism; FTIR; nucleation

INTRODUCTION

Isotactic polypropylenes (iPPs) can present a large variety of interesting microstructures depending in a complex manner on the production conditions (nature of the catalyst and polymerization procedures) and on the processing conditions (thermal history and presence of specific nucleants).[1–14] This complexity is consequence of the wealth of crystalline forms that can be found in iPP. Semicrystalline iPP can present three different crystal modifications named α, β, and γ with monoclinic, trigonal, and orthorhombic cells, respectively. All these crystalline phases are formed by packing identical threefold helices with a 0.65-nm chain axis repeat distance and alternating or identical helical hand. Additionally, a phase of intermediate or mesomorphic order can be found after fast quenching of iPP.[14]

The most common polymorph in iPPs that were obtained using Ziegler–Natta (ZN) catalyst is the α-crystalline phase. The β phase is metastable and can be only found after solidification of ZN-iPP on special conditions or after the addition of adequate nucleating agents.[14,15] The γ phase usually appears intermixed with α crystals in samples of low molecular weight in branched and nonbranched copolymers of iPP and α-olefins and ethylene, respectively, or in samples that were solidified under pressure.[14,16–19] In general, it has been also observed that after isothermal crystallization of ZN ethylene-propylene copolymers at high pressures only the γ form is present.[19]

The conformational and crystalline structure of iPP obtained by using metallocene catalysts, miPP, has been studied in lesser extension. The published results reveal that a mixture of α and γ forms is obtained when the miPPs are crystallized from the melt.[10] The amount of γ form decreases when the isotactic content or the molecular weight increases.[20,21] The relative proportions of α and γ phases are also dependent on cooling rate from the melt: the formation of γ phase is generally favored by slow cooling rates although the content in γ form goes through a maximum.[21] However, some questions as to the effect of the β-nucleants on the conformation and crystalline structure of the iPP obtained by using metallocene catalyst have been only scarcely studied.

Wide-angle X-ray scattering (WAXS) and differential scanning calorimetry (DSC) are the experimental

Correspondence to: V. Lorenzo (vicente.lorenzo@upm.es).
Contract grant sponsor: MEC; contract grant numbers: MAT2007-65519-C02-02, MAT2007-65519-C02-01.
Contract grant sponsor: MICINN; contract grant number: PET2008_0108.

TABLE I
Structural Characterization of the Polypropylene that Was Studied

Sample	MFI (230°C/2.16 kg)	NMR % II	NMR 2.1-*r* (%)	M_w (g/mol)	M_w/M_n
miPP29	28.8	90.3	0.85	207,000	2.37

1,3-regio-errors have not been detected.

MFI reads for melt flow index, %II, for isotacticity as measured by nuclear magnetic resonance (NMR), 2.1-*r* (%), for the percentage of 2–1 regio-irregularities and M_w and M_n, for the weight and number molecular mass averages, respectively.

techniques most used in the study of polymer morphology, providing information about the internal structure. However, other experimental techniques can also provide some useful information. Fourier transform infrared (FTIR) spectroscopy is an experimental technique that is sensitive to the chemical composition, the configuration, the conformation, and the environment of the macromolecular chains. Consequently, FTIR spectroscopy has been systematically used to obtain information about the crystalline structure of iPP.[22] The most interesting absorption bands that can be used for the structural characterization of iPP are localized in the fingerprint region of the IR spectra between 800 and 1400 cm^{-1}. These bands are called regularity or helix bands, because they are due to the intramolecular coupling of vibration modes.[18,23–25] As a result of the experimental work carried out during the past 15 years, several specific bands in the fingerprint region can be related to different values of the critical length "*n*," being "*n*" the minimum number of monomer units in the helical sequences. For example, the appearance of the bands at 973, 998, and 841 cm^{-1} is related to n values of 5, 10, and 12, respectively. In fact, the structural evolution in the crystallization process of iPP has been followed by monitoring these bands in time-resolved FTIR spectroscopy experiments.[24–25] Moreover, the ratio of the intensities of some of these regularity bands has been related to the degree of crystallinity[26] or to the isotacticity.[27] Other authors have related intensity ratios of some of these bands to the β phase content using IR microscopic techniques.[28–30] The above results seem to indicate that the morphology of the different iPPs can be characterized by using FTIR spectroscopy. It has been also proved that the polymorphism of iPP can be studied by means of far infrared spectroscopy, because the splitting of some lines is sensitive to the environment of the macromolecular chains in the crystalline cells.[31]

In this work, different miPP samples were prepared varying the β-nucleant agent content, the cooling rate, and the material used as mold surface. The β-nucleant agent was calcium pimelate.[32] Different specimens were analyzed using WAXS, DSC, and FTIR spectroscopy. The aims of the work are to present some results about the influence of the processing conditions on the crystalline microstructure of miPP and to get a deeper understanding of the utilization of FTIR spectroscopy as a tool for the characterization of these materials.

EXPERIMENTAL

A metallocenic iPP supplied by Basell was used for this study. The melt flow index of this polymer is 28.8 g/min according to the supplier's information and, consequently, it has been named miPP29. The characteristics of this polymer are collected in Table I.

Molecular weights and molecular weight distribution were determined by means of size exclusion chromatography with a Waters 150C equipment connected in line to a viscometer Viscotek 150 R, at 145°C in 1,2,4-trichlorobenzene and with three columns of Polymer Labs (two mixed B of 10 μm and one of 10^{-2} μm). Polystyrene standards were used for calibration.

^{13}C-NMR spectra were obtained at 373 K on a Bruker Avance DPX-300 spectrometer operating at 75.4 MHz. The sample was prepared in 5-mm NMR sample tubes by dissolving the polymer in a mixture of 1,2,4-trichlorobenzene and deuterated *o*-dichlorobenzene.

A full factorial 2^3 experimental design was used to study the influence of the processing variables on the structure of miPP29. The three input factors of the experimental design were the addition of the nucleating agent to the polymer, the rate of cooling from the melt, and the nature of the surface of the mold. Two replications were run at each setting of the input factors.

The two levels for the first of the input factors were the addition of a 0.5 mass percent (high level) or not addition (low level) of the β-nucleating agent. The agent used for the preparation of the β-nucleated samples was calcium pimelate. The nucleator was obtained from a mixture of pimelic acid and calcium stearate (in a 1 : 2 weight ratio) supplied by Fluka that is reported to be a very effective β-nucleator.[33,34] A 0.5-mass percent of this mixture was incorporated into miPP29 by blending in a IMVOLCA 20-25 laboratory extruder, and the extruded product was then cut to granules. To check the homogeneity of the material, some of the granules were melted in the calorimeter: no significant differences were observed among their thermograms. The samples are named A and nA, respectively, for the nucleated and non-nucleated specimens. The nA samples were extruded and chipped

in the same conditions that were used for blending the β-nucleating agent and the miPP29. This procedure equals the effect of the preparing conditions on the microstructure of both materials.

The high level for the second of the input factors of the 2^3 experimental design is denoted with the letter Q and corresponds to a cooling rate close to 100°C/min. This thermal history was applied to the samples by quenching them from the molten state (190°C) to room temperature between the water-cooled plates of a hydraulic Collin press. The low level of the cooling rate, named S, consisted of a slow cooling between the plates after the press was switched off. The average cooling rate resulting in this case is ~ 1.5°C/min. The thicknesses of the specimens that were prepared following this method range around 50 μm.

The miPP29 samples were solidified in contact with either polyester (100-μm thick) or polyimide (UPILEX 75S sheet from Ube Industries, 75-μm thick) mold surfaces. The former material was assigned to the high level of the third input factor, and these samples were labeled PEs, whereas the latter, designated PI, was assigned to the low level.

Consequently, the specimens are identified by means of a three code designation. The first code (A/nA) indicates the addition or not of nucleating agent, the second one (Q/S) is related to the cooling rate, and the third one (PEs/PI) refers to the nature of the mold surface.

The crystallinity levels of these samples and the relative proportions of the different polymorphs were evaluated by means of WAXS techniques. WAXS patterns were recorded in the reflection mode, at room temperature, by using a Bruker D8 Advance diffractometer provided with a Goebel mirror and a PSD Vantec detector (from Bruker, Madison, Wisconsin). Cu Kα radiation (λ = 0.1542 nm) was used, operating at 40 kV and 40 mA. The equipment was calibrated with different standards. The diffraction scans were collected within the range of 2θ from 3 to 40° with a 2θ step of 0.024° and 0.2 s per step.

The thermal behavior of the eight samples was analyzed by DSC by using a modulated TA Instruments DSC Q100 DSC connected to a cooling system and calibrated with different standard. The sample weights were around 0.6 mg. The melting curves were recorded at a rate of 20°C/min.

Two different FTIR spectrophotometers, a Mattson 3020 and a Perkin-Elmer 1600, were used to obtain the transmission IR spectra of the samples. In the two cases, the spectra of the materials were measured at room temperature in transmission mode, with resolution 4 cm^{-1}, using the 50-μm thick films obtained in the Collins press as described above. Each spectrum was the coaddition of 25 scans.

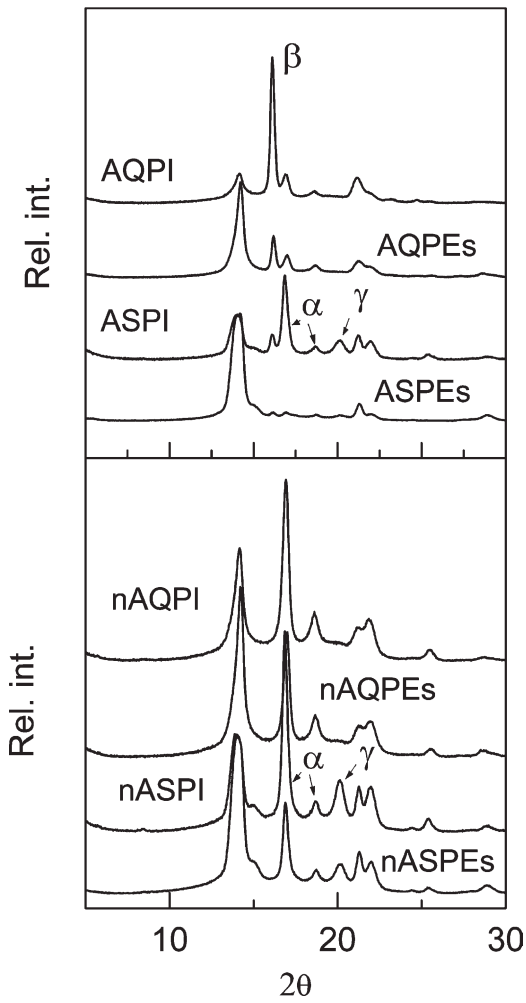

Figure 1 X-ray diffractograms of the eight miPP29 samples that were studied.

Before the measurement of the intensities, baseline correction of the original spectra was carried out using Omnic 7.0 software. The same results were obtained with the two spectrometers.

RESULTS AND DISCUSSION

X-ray analysis

The eight samples prepared according to the method described previously were characterized by means of WAXS. The diffractograms for all the samples are collected in Figure 1. The X-ray determinations of the degree of crystallinity were performed after subtraction of the corresponding amorphous component by comparison with the totally amorphous profile of an elastomeric PP sample.[35] These corrected diffractograms were used to determine the proportions of the different crystalline phases by performing the deconvolution into all the different diffraction peaks corresponding to each polymorph. It has been proved[36] that this method is more precise than the

TABLE II
Mass Fractions of the Amorphous Phase, f_a^{WAXS}, and of the α, β, and γ Polymorphs Determined by Wide-Angle X-Ray Scattering

Sample	f_a^{WAXS}	Fraction of each crystalline form		
		α	β	γ
AQPEs	0.30	0.48	0.09	0.13
AQPI	0.28	0.19	0.44	0.09
ASPEs	0.25	0.31	0.01	0.43
ASPI	0.22	0.24	0.05	0.49
nAQPEs	0.34	0.52	0	0.14
nAQPI	0.31	0.54	0	0.15
nASPEs	0.32	0.22	0	0.46
nASPI	0.28	0.20	0	0.52

previously used, due to Turner-Jones et al.,[4] because the calculations involve all available diffraction peaks instead of using only the most intense ones. The proportions of the different phases that can be found in miPP29 are presented in Table II.

Regarding the addition of the nucleating agent, two different effects are observed. On the one hand, the crystallinity level as determined from X-ray diffraction experiments, f_a^{WAXS}, is around 5% higher for the samples with agent (Axx) than for the corresponding samples without agent (nAxx). On the other hand, β phase is only present in nucleated samples. Both results agree with other previously reported for iPPs, and they can be explained in terms of the heterogeneous nucleation effect of the agent.[37]

The analysis of the results in Table II can also provide information about the influence of the cooling rate on the microstructure of these samples. As can be expected, the crystallinity levels of the slowly cooled samples (xSx) are higher than those of the corresponding quenched samples (xQx) with differences that range from 2 to 5%. The experimental results also illustrate the effect of the cooling rate in the competition among the different polymorphs of iPP. It can be observed that the proportion of γ phase increases when the cooling rate decreases. The same result has been previously obtained for other metallocenic iPP,[20,36] for iPP synthesized with very lowly isospecific Ziegler–Natta catalyst and for iPP copolymers with α-olefins.[17,19] According to Alamo et al.,[21] the maximum of the relative percentage of γ phase is related to the average length of isotactic sequences and can reach an asymptotic value of around 80%. The results in Table II show that the percentage of γ phase relative to crystallinity level reaches a maximum value around 70% for nASPEs and nASPI samples. This value is close to the greatest relative percentages of γ phase that were reported for other miPPs.[17,20,36]

Table II also shows some interesting results related to the influence of the nature of the mold surface on the structure of the miPP samples. The global crystallinity levels of the samples that were molded in contact with PI films are around a 3% higher than those of samples molded in contact with PEs films. This result seems to point to the fact that the PI surface has a higher ability than the PEs surface for nucleating heterogeneously the crystalline phases of miPP29. Moreover, the difference on the nucleating capacity of these mold surfaces is selective about the polymorphs of miPP and, consequently, the nature of the mold surface also affects very much the competition between the different crystalline phases.

The analysis of the results obtained with the nAxx samples shows that the ratios of the α to the γ phase contents are 3.7 and 0.4 for the Q and S specimens, respectively. These values are similar to those calculated from the results reported in the literature for slow cooled and quenched from the melt miPP samples in contact with plates of nonreferenced nature.[17,36] Consequently, it can be stated that the proportion of the α to the γ phase contents for the miPP non-nucleated samples is insensitive to the nature of the mold. However, results that were obtained for the Axx samples clearly suggest that the quantity of the β-polymorph depends on the nature of the molds. It can be seen that the ratio of β-phase content on the AxPI sample to that on the AxPEs samples is close to 5.

It is important to remark that the γ phase content of the nAxx specimens is similar to that of the corresponding Axx films and, thus, it can be stated that the γ phase content of this miPP is independent of the nature of the mold and of the addition of β-nucleating agent. Thus, the analysis of Table II results shows that the γ phase content is 0.13 ± 0.03 and 0.49 ± 0.03 for the xQx and xSx miPP29 samples, respectively. This value seems to depend uniquely on the cooling rate. However, the competition between the α and β polymorphs measured by the ratio of the respective mass fractions is controlled by the cooling rate and by the nature of the mold. These results show that the mold surface can enhance considerably the β-nucleant effect of the agent.

Some years ago, Varga stated that "It is worth noting that no beta-transcrystalline microstructure has been found to date, since this would require the presence of a surface having selective beta-nucleating activity."[37] The surfaces studied in this work do not have intrinsic β-nucleating activity, which do not promote the β-polymorph in non-nucleated miPPs, but they play a significant role in the activity of some β-nucleant agents and, hence, on the final morphology of the β-nucleated miPPs.

As the surface effect is usually confined to a narrow layer close to the surface of the samples, the

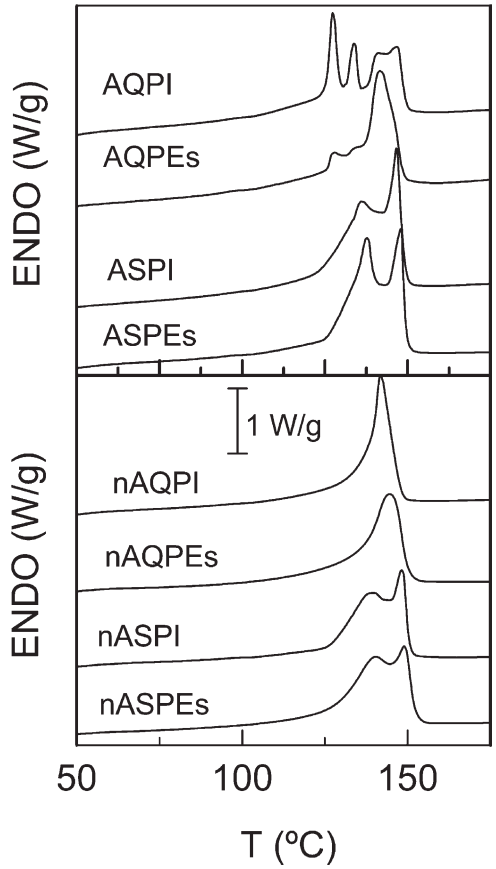

Figure 2 DSC curves corresponding to the nucleated (top) and the non nucleated (bottom) samples.

relative importance of the above phenomenon increases as the thickness of the specimen decreases. In fact, this effect that is easily detectable in the studied samples because their reduced thicknesses can be of interest to economize expensive nucleant agents in the production of films of miPP with high content of β-phase.

DSC melting curves

Similar conclusions about the nature of the crystalline phases that can be found in the different samples are deduced from the DSC melting curves that are presented in Figure 2. The thermograms of the nASxx samples show two distinctive contributions centered at around 140 and 149°C. The relative magnitudes of these endotherms, assigned to the melting of the γ and α phase, respectively,[35] confirm that the γ phase is the main polymorph in these samples. On the contrary, the melting curves of the nAQxx samples display a peak centered around 149°C and a small shoulder that appears around 140°C, reflecting that the most abundant crystalline phase is now the α polymorph.

The thermogram of the AQPI sample displays two very intense and narrow peaks, at around 130 and 135°C arising from the melting and recrystallization of the β crystals. These peaks can be also observed in the AQPEs thermogram, but their intensities are lower. This fact reflects the very important enhancement of the β-polymorph content due to the nature of the mold surface that was described previously in the analysis of the X-ray diffraction experiments. The contribution of the β phase appears like a shoulder in the melting curves of the ASxx samples.

These thermograms cannot be used for assessing the relative proportions of the different crystalline phases due to the transformations that the β modification undergoes during the heating process. Anyway, there is a qualitative agreement between the results of these experiments and those of determination of the structure by means of X-ray diffraction.

FTIR analysis

Figure 3 shows the FTIR spectra of the AQPEs and nAQPEs samples obtained with the Matson spectrophotometer. These spectra have been normalized using the band centered at 1460 cm^{-1} as internal reference. The normalized values of the intensity of the bands are named $I_S(\nu)$ where subscript S indicates the sample code and ν represents the wavenumber expressed in cm^{-1}. As it can be expected, both spectra are very similar because FTIR spectroscopy is mainly sensitive to internal vibrations of the macromolecular chains and the unit cells of the polymorphs of iPP correspond to different packings of identical 3_1 helices. However, a detailed exam allows one to detect small differences like those that are presented in the amplification at the bottom part of Figure 3, which appears to indicate that the FTIR spectra in this region is dependent on the morphology of the miPPs. Such a relationship between the infrared spectra and the structure of the polymer would be of great interest, because the infrared spectroscopic techniques are fast and not expensive.

To verify if these differences are significant and are related to structural details, the spectra were studied by means of multivariate data analysis techniques,[38] a tool that has been previously applied to the analysis of the FTIR spectra of polypropylenes.[39] The infrared data were analyzed using the WAXS data to calibrate and evaluate the relationship between the FTIR spectra and the structure of the miPPs. The partial least square PLS2 algorithm was used, because it is an adequate method to study problems with a high degree of colinearity and several dependent variables.[40,41] This algorithm was coded by using the open source platform for numerical computation SCILAB 5.1.1 (www.scilab.org). The samples AQPI, ASPEs, nAQPEs, and nASPI were selected for calibration of the model, and the

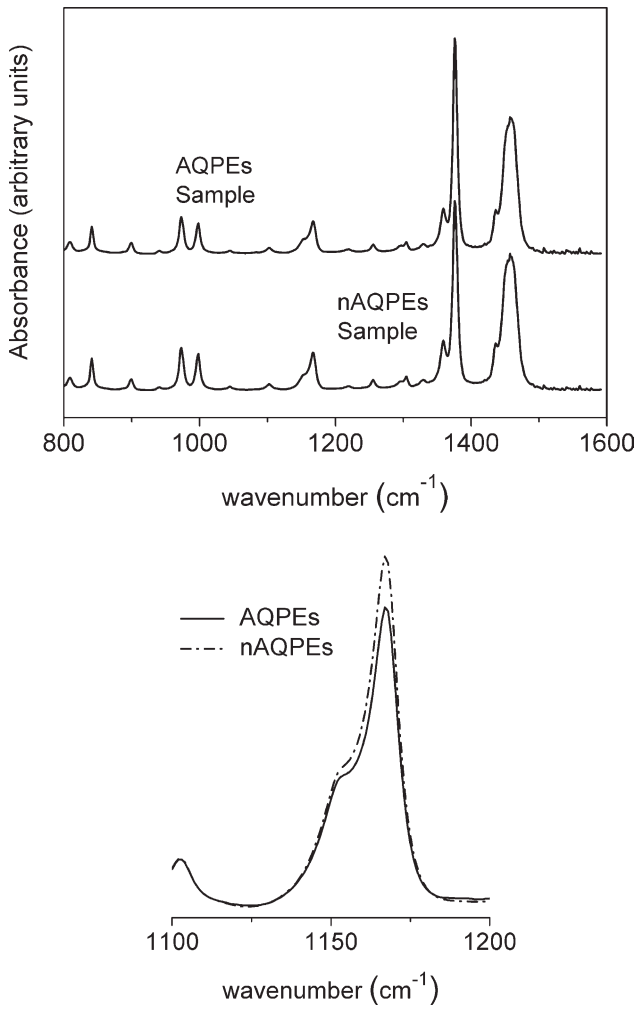

Figure 3 FTIR spectra of the AQPEs and nAQPEs samples that were normalized using the 1460 cm^{-1} band as internal reference. The lower part of the figure shows the differences between both spectra in the 1100–1200 cm^{-1} region.

other ones were used as the validation set. The wavenumber interval that was considered for the PLS2 analysis ranges from 1350 to 750 cm^{-1}, because the bands of this region are regularity bands, sensitive to the microstructure of the specimens. In fact, it has been proved that some of these absorbance bands are related to the length of the 3_1 helical sequences[18,24] and that some intensity ratios in this region can be related to the proportions of the different polymorphs in iPPs.[29] These calculations were applied to the spectra obtained with both spectrometers, and the calculated fractions of the different polymorphs were the same for both sets of data. This identity allows one to gain confidence in our experimental work. To validate the number of principal components that were selected, the cumulative proportion of the total variance accounted for by the model was estimated, and values greater than 90% were obtained for the percentage of explained variation.

The phase proportions of the miPPs calculated using the FTIR are collected in Table III. The comparison of these calculated values with those of Table II shows a reasonable agreement between the FTIR and the WAXS results. As the difference between the values in both Tables can be explained in terms of the small number of calibration and validation samples, it can be concluded that FTIR spectroscopy in an adequate experimental technique to obtain quantitative information about the polymorphism of miPP.

An alternative approach for the interpretation of FTIR spectra is the comparison of the intensities of selected bands. The peaks considered in this work to compare the spectra of the different miPP29 samples are the regularity bands centered at 940, 1220, 1167, 1303, 1330, 841, 998, 900, 808, 1100, and 973 cm^{-1}. The appearance of these bands has been related to different values of the minimum number of monomer units in the helical sequences of iPP.[24] Several authors have related previously the intensities of these bands, or their ratio, to the morphology of different iPP. Thus, the ratio of the intensities of the bands at 998 and 973 cm^{-1}, $I_S(998)/I_S(973)$, has been reported to be dependent on the isotacticity or the degree of crystallinity[24,26,20,42] and the ratio $I_S(1330)/I_S(1167)$ has been related to the content of the β-polymorph.[29] At this point, it is important to remark that the intensity of many bands of the FTIR spectra of iPP are influenced by the details of thermal and mechanical history and, consequently, only samples that have been processed in a similar way must be compared.

The differences in the regularity bands were analyzed using analysis of variance techniques. The significance of the main effects of the experimental variables on the intensities of the regularity bands and on the ratios of intensities related to crystallinity and polymorphism of iPP is collected in Tables IV and V.

The absorbance of some of the regularity bands depends on the addition of the β-nucleating agent, which can be seen in Table IV. Figure 3 shows that

TABLE III
Mass Fractions of the Amorphous Phase, f_a^{FTIR}, and of the α, β, and γ Polymorphs Calculated by Partial Least Square Regression (the Results Have Not Been Corrected to Avoid Negative Values)

Sample	f_a^{WAXS}	Fraction of each crystalline form		
		α	β	γ
AQPEs	0.28	0.34	0.13	0.25
ASPI	0.27	0.17	0.09	0.47
nAQPI	0.29	0.49	0.02	0.20
nASPEs	0.29	0.31	−0.04	0.44

TABLE IV
Significance of Addition of β-Nucleating Agent, Cooling Rate, and the Nature of the Mold on the Intensities of the Regularity Bands

Wavenumber (cm^{-1})	Addition of agent	Cooling rate	Nature of the mold
940	×	×	✓
1220	×	×	✓
1167	✓	×	✓
1303	×	×	✓
1330	×	×	✓
841	×	×	×
998	✓	×	×
900	×	×	×
808	×	×	×
1100	×	×	×
973	×	×	×

The ✓ and × symbols read for a significant and a non-significant factor, respectively (confidence level: 95%).

the intensity of the 1167 cm^{-1} band is significantly lower in the nucleated samples than in the corresponding non-nucleated specimens. This result probably reflects the effect of reduction of the size and the perfection of the crystallites due to the heterogeneous nucleation that was induced by the agent.

According to Table IV, the intensities of the regularity bands that correspond to the longest helix lengths of isotactic sequences (940, 1220, 1167, 1303, and 1330 cm^{-1}) are sensitive to the nature of the mold. Figure 4 illustrates the influence of the nature of the mold surface on the intensities of two of these bands and shows that 940 and 1220 bands are significantly more intense for xxPEs samples than for xxPI specimens. This influence could be explained in terms of a heterogeneous nucleation effect of the PI molds: the higher crystallinity of the xxPI samples is achieved by a higher nucleation frequency and, consequently, the crystalline entities are smaller and the regularity of the chain folding is lower.

As mentioned above, the ratio $I_s(998)/I_S(973)$ has been related to isotacticity and degree of crystallinity of ZN-iPP samples with predominant, if not unique,

TABLE V
Significance of the Addition of β-Nucleating Agent, the Cooling Rate, and the Nature of the Mold on the Intensity Ratios of Bands that Have Been Reported as Been Related to Crystallinity and to the Content of the β Polymorph in the Literature

Intensity ratio	Addition of agent	Cooling rate	Nature of the mold
998/973	✓	✓	×
1256/1168	×	✓	×
1296/1305	×	×	×
1330/1168	✓	×	✓

The ✓ and × symbols read for a significant and a non-significant factor, respectively (confidence level: 95%).

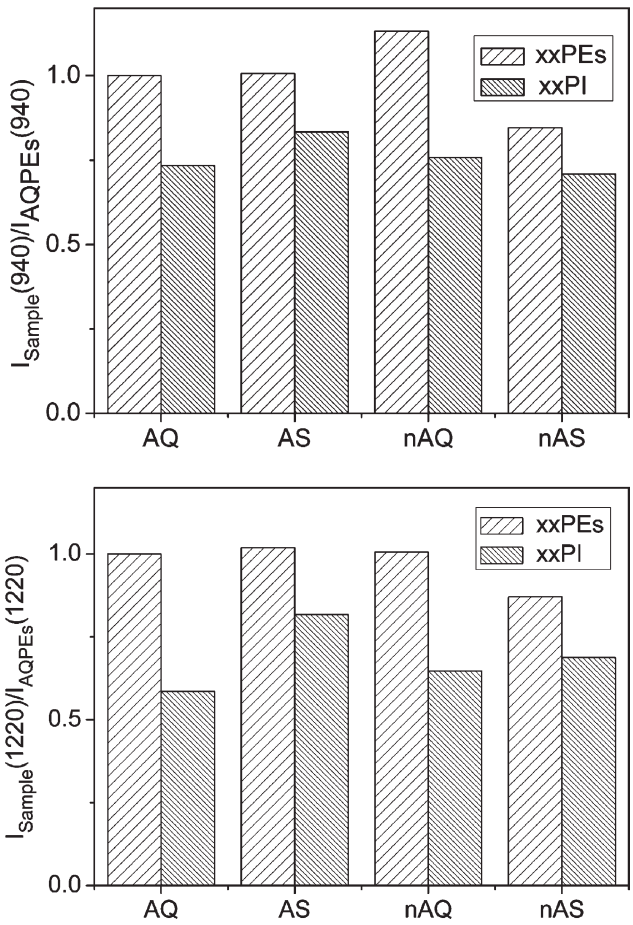

Figure 4 Influence of the nature of the mold surface on the normalized intensities of the bands centred at 940 and 1220 cm^{-1}, $I_S(\nu)$, for the different samples.

α crystals. The interpretation of this ratio for miPP samples is expected to be more complex because of the influence of the polymorphism. Figure 5 illustrates the effect that the cooling conditions of samples solidified in contact with the same mold surface and identically nucleated have on the value of this quotient. As it can be expected, the value of this ratio for the xSx samples is greater than for the corresponding xQx ones, reflecting the dependence of the global crystallinity level on the cooling rate. More interesting results are obtained when the effect of the nucleating agent addition is considered. Figure 6 clearly shows that the points that describe the behavior of Axx and the nAxx samples fit different lines. It can be seen that the value of the $I_S(998)/I_S(973)$ ratio is higher for non-nucleated samples than for nucleated samples with the same degree of crystallinity. If, as it has been postulated, this ratio is related to the microstructural order, the results in Figure 6 probably point to the greater perfection and regularity of the crystallites of the non-nucleated samples.

Figure 7 shows the influence of the addition of β-nucleant agent on the ratio of the intensity of the

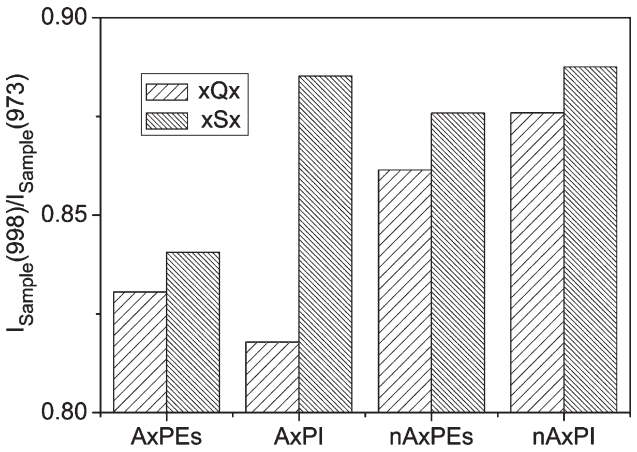

Figure 5 Ratio between the intensities of the 998 and 973 cm^{-1} FTIR bands for quenched (xQx) and slow cooled (xSx) samples.

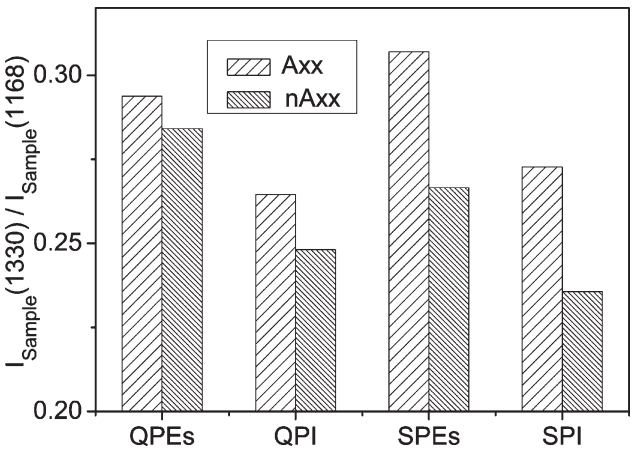

Figure 7 Effect of the addition of the nucleating agent on the ratio between the intensities of the 1330 and 1168 cm^{-1} FTIR bands.

1330 cm^{-1} band to that of the 1167 cm^{-1} one. It can be seen that the values of the quotient $I_S(1330)/I_S(1167)$ are greater for nucleated samples than for the corresponding non-nucleated ones. These results agree with those previously reported by Ellis et al.,[29] which have stated, using IR microscopy, that this ratio is related to the content of the β-polymorph.

CONCLUSIONS

The two main conclusions that can be drawn from the previous analysis are as follows:

On the one hand, our experimental results show that FTIR spectroscopy is an adequate tool for studying polymorphism of miPP. Using multivariate analysis techniques and calibration against WAXS data, it has been proved that it is possible to calculate the proportions of the different crystalline forms from the FTIR spectra. The analysis of the intensities of selected regularity bands also gives useful information about the morphology of miPPs.

On the other hand, it has been found that films of β-nucleated miPPs crystallized between polyimide films show a much higher content in the β polymorph than those prepared between polyester films. The obtained results seem to indicate that the mold surface can play a significant role in the activity of some β-nucleant agents and, hence, it can determine the final morphology of the β-nucleated miPPs. This can be of interest to economize expensive nucleant agents in the production of films of miPP with high content of β phase.

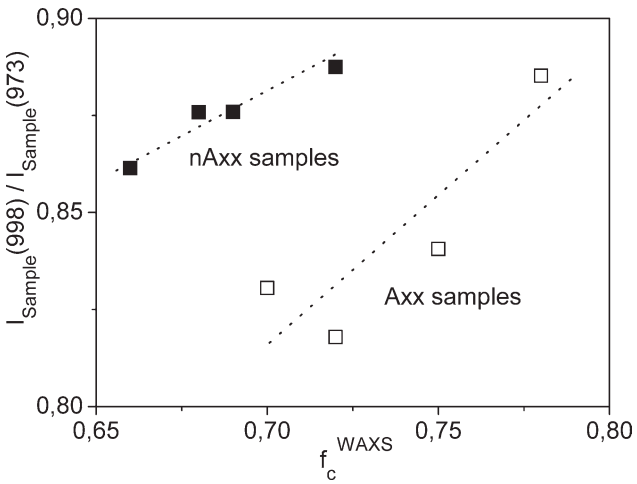

Figure 6 Relationship between the degree of crystallinity measured by means of WAXS and the ratio between the intensities of the 998 and 973 cm^{-1} FTIR bands for nucleated (Axx) and non-nucleated (nAxx) samples. The lines are just guides to the eye.

References

1. Brückner, S.; Meille, S. V.; Petraccone, V.; Pirozzi, B. Prog Polym Sci 1991, 16, 361.
2. Phillips, P. J.; Mezghani, K. In The Polymeric Materials Encyclopedia; Salamone, J. C., Ed.; CRC Press: Boca Raton, 1996; Vol.9, p 6637.
3. Natta, G.; Corradini, P. Nuovo Cimento Suppl 1960, 15, 40.
4. Turner-Jones, A.; Aizlewood, J. M.; Beckett, D. R. Makromol Chem 1964, 75, 134.
5. Brückner, S.; Meille, S. V. Nature 1989, 340, 455.
6. Varga, J. J Mater Sci 1992, 27, 2557.
7. Meille, S. V.; Ferro, D.; Brückner, S.; Lovinger, A. J.; Padden, F. J. Macromolecules 1994, 27, 2615.
8. Kissel, W. J.; Han, J. H.; Meyer, J. A. In Handbook of Polypropylene and Polypropylene Composites, Revised and Expanded, 2nd ed.; Karian, H. G., Ed.; New York: Marcel Dekker, 2003; pp 11–34.
9. Maier, C.; Calafut, T. Polypropylene, The Definitive User's Guide and Databook; Plastics Design Library: Norwich, NY, 1998.
10. Imanishi, Y.; Naga, N. Prog Polym Sci 2001, 26, 1147.
11. Zhang, P.; Liu, X.; Li, Y. Mater Sci Eng A Struct 2006, 434, 310.
12. Thomann, R.; Semke, H.; Maier, R. D.; Thomann, Y.; Scherble, J.; Mulhaupt, R.; Kressler, J. Polymer 2001, 42, 4597.

13. Van der Burgt, F. P. T. J.; Rastogi, S.; Chadwick, J. C.; Rieger, B. J Macromol Sci B 2002, 41, 1091.
14. Lotz, B.; Wittmann, J. C.; Lovinger, A. J. Polymer 1996, 37, 4979.
15. Varga, J.; Ehrenstein, G. W. In Polypropylene. An A-Z reference. Karger-Kocsis, J., Ed.; Kluwer Academic Publishers: Dordrecht, 1999; pp 51–59.
16. Kressler, J. In Polypropylene. An A-Z reference. Karger-Kocsis, J.; Ed.; Kluwer Academic Publishers: Dordrecht, 1999; pp 267–272.
17. Pérez, E.; Zucchi, D.; Sacchi, M. C.; Forlini, F.; Bello, A. Polymer 1999, 40, 675.
18. Su, Z.; Wang, H.; Dong, J.; Zhang, X.; Dong, X.; Zhao, Y.; Yu, J; Han, C. C.; Xu, D.; Wang, D. Polymer 2007, 48, 870.
19. Dimeska, A.; Philips, P. J. Polymer 2006, 47, 5445.
20. Arranz-Andrés, J.; Peña, B.; Benavente, R.; Pérez, E.; Cerrada, M. L. Eur Polym J 2007, 43, 2357.
21. Alamo, R. G.; Kim, M. H.; Galante, M. J.; Isasi, J. R.; Mandlekern, L. Macromolecules 1999, 32, 4050.
22. Andreassen, E. In Polypropylene. An A-Z reference. Karger-Kocsis, J.; Ed.; Kluwer Academic Publishers: Dordrecht, 1999; pp 320–328.
23. Kissin, Y. V.; Rishina, L. A. Eur Polym J 1976, 12, 757.
24. Zhu, X.; Yan, D.; Fang, Y. J Phys Chem B 2001, 105, 12461.
25. Reddy, K. R.; Tashiro, K.; Sakurai, T.; Yamaguchi, N.; Sasaki, S.; Masunaga, H.; Masaki, T. Macromolecules 2009, 42, 4191.
26. Schönherr, H.; Wiyatno, W.; Frank, C. W.; Fuller, G. G.; Gast, A. P.; Pople, J. A.; Waymouth, R. M. Macromolecules 2002, 35, 2654.
27. Burfield, D. R.; Loi, P. S. T. J Appl Polym Sci 2003, 36, 279.
28. Ellis, G.; Gómez, M.; Marco, C. Int J Vibr Spec 2001, 5, 7; Available at: www.ijvs.com.
29. Ellis, G.; Marco, C.; Gómez, M. Infrared Phys Technol 2004, 45, 349.
30. Ellis, G.; Marco, C.; Gómez, M.; Blancas, C. Bol Soc Esp Ceram V 2004, 43, 340.
31. Beckett, D. R.; Chalmers, J. M.; Mackenzie, M. W.; Willis, H. A.; Edwards, H. G. M.; Lees, J. S.; Long, D. A. Eur Polym J 1985, 21, 849.
32. Li, X.; Hu, K.; Ji, M.; Huang, Y.; Zhou, G. J Appl Polym Sci 2002, 86, 633.
33. Shi, G.; Zhang, X.; Qiu, Z. Makromol Chem 1992, 193, 583.
34. Varga, J.; Mudra, I.; Ehrenstein, G. W. J Appl Polym Sci 1999, 74, 2357.
35. Mansel, S.; Pérez, E.; Benavente, R.; Pereña, J. M.; Bello, A.; Roll, W.; Kirsten, R.; Beck, S.; Brintzinger, H. H. Macromol Chem Phys 1999, 200, 1292.
36. Krache, R.; Benavente, R.; López-Majada, J. M.; Pereña, J. M.; Cerrada, M. L.; Pérez, E. Macromolecules 2007, 40, 6871.
37. Varga, J. In Polypropylene. Structure, blends and composites, Vol. 1. Karger-Kocsis, J., Ed.; Chapman&Hall: London, 1995; pp 56–115.
38. Peña, D. Análisis de Datos Multivariantes; McGraw-Hill: Madrid, Spain, 2002.
39. Pandey, G. C.; Kumar, A.; Garg, R. K. Eur Polym J 2002, 38, 745.
40. Jørgensen, B.; Goegebeur, Y. STO2: Multivariate Data Analysis and Chemometrics; Available at: http://statmaster.sdu.dk/courses/STO2/module08/index.html, 2007. Accessed on 30 December.
41. Höskuldsson, A. J Chemometrics 1988, 2, 211.
42. Lamberti, G.; Brucato, V. J Polym Sci B Polym Phys 2003, 41, 998.